IMPROVING ENERGY EFFICIENCY VIA OPTIMIZED CHARGE MOTION AND SLURRY FLOW IN PLANT SCALE SAG MILLS

ANNUAL REPORT

Reporting Period Start Date: 22 July 2003
Reporting Period End Date: 21 July 2004

Raj K Rajamani, Project Manager
Sanjeeva Latchireddi, Project Leader
Sravan K Prathy, Graduate Student
Trilokyanath Patra, Graduate Student

December 2005

DE-FC26-03NT41786

University of Utah
135 S 1460 E Room 412, Salt Lake City 84112

DISCLAIMER

ABSTRACT

The U.S. mining industry operates approximately 80 semi-autogenesis grinding mills (SAG) throughout the United States. Depending on the mill size the SAG mills draws between 2 MW and 17 MW. The product from the SAG mill is further reduced in size using pebble crushers and ball mills. Hence, typical gold or copper ore requires between 2.0 and 7.5 kWh per ton of energy to reduce the particle size. Considering a typical mining operation processes 10,000 to 100,000 tons per day the energy expenditure in grinding is 50 percent of the cost of production of the metal.

A research team from the University of Utah is working to make inroads into saving energy in these SAG mills. In 2003, Industries of the Future Program of the Department of Energy tasked the University of Utah team to build a partnership between the University and the mining industry for the specific purpose of reducing energy consumption in SAG mills. A partnership was formed with Cortez Gold Mines, Kennecott Utah Copper Corporation, Process Engineering Resources Inc. and others.

In the current project, Cortez Gold Mines played a key role in facilitating the 26-ft SAG mill at Cortez as a test mill for this study. According to plant personnel, there were a number of unscheduled shut downs to repair broken liners and the mill throughput fluctuated depending on ore type. The University team had two softwares, Millsoft and FlowMod to tackle the problem. Millsoft is capable of simulating the motion of charge in the mill. FlowMod calculates the slurry flow through the grate and pulp lifters. Based on this data the two models were fine-tuned to fit the Cortez SAG will.

In the summer of 2004 a new design of shell lifters were presented to Cortez and in September 2004 these lifters were installed in the SAG mill. By December 2004 Cortez Mines realized that the SAG mill is drawing approximately 236-kW less power than before while maintaining the same level of production.

In the first month there was extreme cycling and operators had to learn more. Now the power consumption is 0.3-1.3 kWh / ton lower than before. The actual SAG mill power draw is 230-370 kW lower. Mill runs 1 rpm lesser in speed on the average. The re-circulation to the cone crusher is reduced by 1-10%, which means more efficient grinding of critical size material is taking place in the mill. All of the savings have resulted in reduction of operating cost be about $0.023-$0.048/ ton.

TABLE OF CONTENTS

1. INTRODUCTION

There are a number of SAG mills in operation around the world whose diameter reaches up to 40 ft. These operations continually invest in new technologies to improve their energy efficiency and capacity in their SAG circuit. Commercial SAG mill performance is determined by a large number of variables, both mine site variables and mill variables. In many cases these variables dictate production capacity seemingly randomly. Therefore a number of operating philosophies, each specific to a plant, have arisen. In almost all concentrators the SAG operation is a continually evolving operation. Every year, ways and means are sought to increase capacity, decrease energy consumption and prolong lifter and liner life. Ore blending, newer designs of lifters, recycle crushing and redesign of grates and trommel screens are a few routes taken at considerable expense.

1.1 Operation of SAG Mills

The processing capability of a semi-autogenous (SAG) mill is greatly affected by ore geology and operating variables within the mill. The key issues can be broadly classified in to two categories: field of breakage/ charge motion and flow through the grate and pulp lifters. The field of breakage and charge motion is primarily affected by the design of shell lifters and mill speed. Once the ore is ground to a size that can pass through the grate holes, the slurry flows into the pulp lifter chamber that transports into the discharge trunnion. These components of the SAG mill are schematically shown in Figure 1.1 for easier understanding.

Once the slurry has made its way via the grinding media charge, its first stage of discharge is via the grates. Hence in the absence of any subsequent restriction the maximum flow capacity that can be obtained for a given mill is determined by the grate design. Here the design variables are open area and radial distribution of slots. The driving force for slurry transport from the mill shell through the grate holes is the difference in pressure head across the grate.

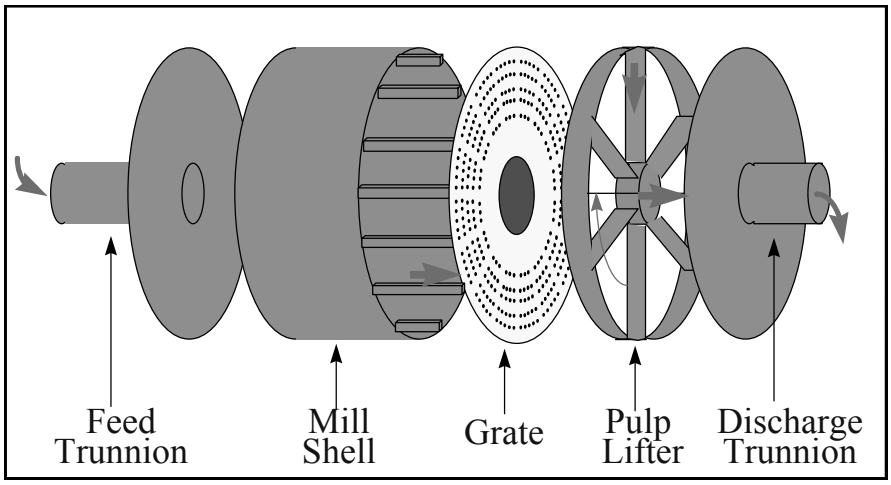

Figure 1.1: Schematic of a typical SAG mill.

1.1.1 **Field of breakage**: The motion of charge or rocks and balls in SAG mils can be viewed as a field of breakage generated as a result of the internal profile of the lifters and the rotational speed of the mill shell. The ore entering through the feed port is ground by this field and, after being sufficiently ground to the grate slot size, the slurry leaves through the slots in the grate. The field of breakage influences the rock mass in the SAG mill. Should the incoming ore be harder and the field of breakage insufficient to reduce the size, the ore stays in the mill longer since it is unable to pass through the grate. The net effect is an increase in rock mass, and the feed rate to the mill must be decreased appropriately to maintain rock to ball ratio. On the other hand, when the ore is soft, the field of breakage reduces the ore size rapidly and hence the rock mass decreases. To sustain a set rock mass, the feed rate must be increased. The complicating factor is that the incoming ore feed itself determines the breakage field.

1.1.2 **Flow through the grate and pulp lifters**: Discharge grates and pulp lifters play an important role in performance of the autogenous and semi-autogenous mills. The performance of the pulp lifters in conjunction with grate design determines the flow capacity of these mills. The function of the pulp lifters is simply to transport the slurry passing through the discharge grate into the discharge trunnion. Its performance depend on the size and design, the grate design and mill operating conditions such as mill speed and charge level. The difficulties associated with slurry transportation from SAG mills have become more apparent in recent years with the increasing trend to build larger diameter mills for grinding high tonnages. This is particularly noticeable when SAG mills are run in closed circuit with classifiers such as fine screens or hydrocyclones.

The performance analysis of conventional pulp lifter designs shows that a large amount of slurry flows back from the pulp lifter into the mill. The flow back depends on the size and design of the pulp lifters. Since the back face of the pulp lifter is the grate itself, the slurry readily flows back into the mill. Subsequently, the field of breakage diminishes when excessive slurry builds in the mill.

1.1.3 **Charge motion**: In a concentrator, all of the auxiliary equipment-pumps, conveyers, screens and hydrocyclones - and two primary resources-steel and electricity-serve primarily to maintain grinding action in the belly of the SAG mill. It is this action that dictates capacity. This being the case, it is understandable to observe this grinding action continuously from the control room and take whatever steps are necessary to keep the grinding field at its highest potential. Unfortunately, the grinding environment within the mill shell is very severe and none of the on-line instrumentation developed so far is able to survive the continuous impact of large steel balls. Since direct observation is impractical, the next available option is a simulation of the grinding field to gauge the intensity of grinding or lack of intensity of grinding.

1.1.4 **Mill power draft**: The field of breakage and flow through grates and pulp lifters influences each other and the net effect is the build-up of a hold-up level in the mill, which draws a certain power and this power draft is clearly linked with mill throughput. If the interaction can be understood then mill capacity can be understood much more clearly. Then the expectation of increasing capacity at the same level of power draft by one means or another can be safely evaluated.

The power draft of a SAG mill and its consequences are illustrated in Figure 1.2, wherein five days of operating data in a 32x14 ft SAG mill is plotted. The power draft of the mill is held between 6 and 7 MW, whereas tons per hour (TPH) of ore feed to the mill shows wide variations between 1000 tph to 1600 tph. When closely examining Figure 1.2, one finds that the feed rate drops whenever the power draft shows an increasing trend, whereas intuitive reasoning says that feed rate should be proportional to power draft.

The data shows that the specific energy consumption (kWh/tonne) of ore is not steady, as one would expect for a typical ore body. Even within a 24-hour time frame, where the feed ore hardness may be assumed constant, the variation in feed rate is drastic. The internal dynamics within the SAG mill, as exemplified by the three broad concepts, are causing wide fluctuations in grinding rate, which in turn is reflected as capacity.

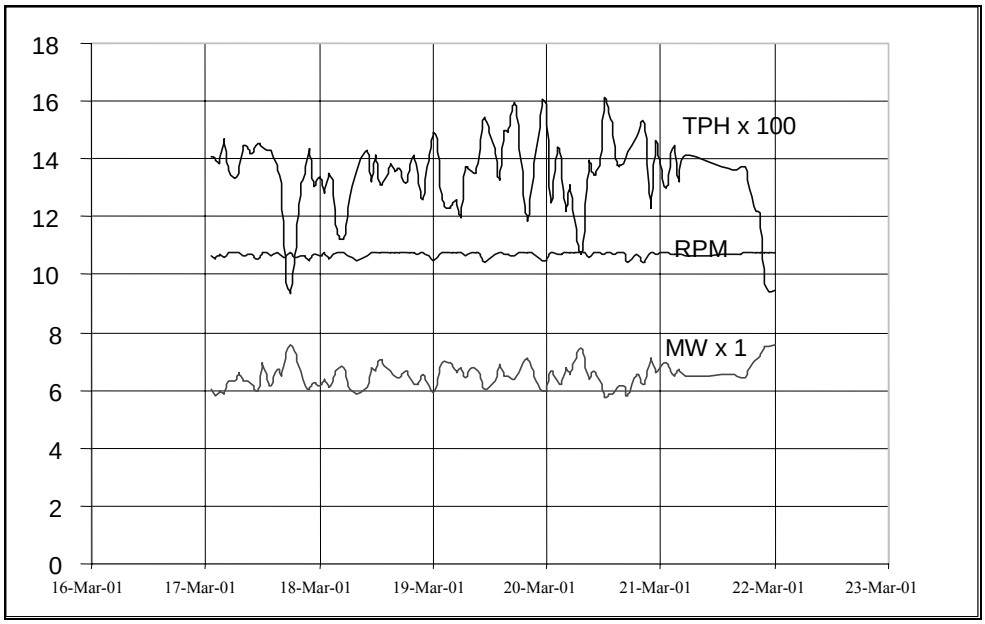

Figure1.2: Five days of plant operating data: 32x14 ft SAG circuit.
(TPH-fresh feed rate, MW-mill power in megawatts)

1.2 **SAG Mill Efficiency**

The energy efficiency of tumbling mills can be directly examined by looking at the motion of ore and grinding balls inside the mill. The make-up of the charge and the lifter bars attached to the inside of the mill shell can be designed particularly to maximize the mass of ore fractured per unit of energy spent. At the same time, the unnecessary collisions of steel balls against the mill shell can be reduced. Furthermore, the cascading charge flow can be altered in such a way as to maximize grinding efficiency. First, the shell lifters are designed in such a way the motion is fully cascading and that part of cateracting motion is made to strike in the vicinity of the toe. In such a charge motion regime both shearing action and impacts are fully utilized in grinding the ore.

The shell lifters are usually replaced once or twice a year. Pulp lifters survive two or three years. The design of these two important mill components has been largely based on trial and error and hence varies considerably between manufacturers. However over the years, important tools such as Millsoft™ and FlowMod™ have begun to help the designers to analyze and understand the influence of the internal components of SAG mills – shell lifters, grate and pulp lifters respectively. The following sections will discuss the basic principles and application of these two simulators.

Project Objectives

The overall objective of the project is to develop an integrated process model to enable the SAG mills to operate with high energy efficiency.

Phase 1:

To study the effect of individual variables such as charge filling, shell lifter configuration and design of discharge grate and pulp lifter on power draft of the mill by isolating the effect of one on each other.

Phase 2:

Conduct plant surveys at Kennecott Utah Copper Corporation and Cortez Gold Mines around the plant scale SAG mills to collect the operational data to simulate in pilot mill to optimize the performance of SAG mill and increase the energy efficiency.

2. EXECUTIVE SUMMARY

Many large mining operations around the world have one or more semi-autogenous (SAG) mills doing bulk of the work in their size reduction operation. The SAG mill is usually followed by a ball mill to finish the size reduction prior to the concentration step. In the past when primary, secondary and tertiary crushers fed material directly to large ball mills, the energy efficiency of the concentrator was determined for the most part by the ball mill operation, whereas now the energy efficiency of a plant often rests largely on the SAG mill operation. This has caused a shift of interest in optimization from ball mills to SAG mills.

Commercial SAG mill performance is determined by a large number of variables, both mine site variables and mill variables. In many cases these variables dictate production capacity seemingly randomly. Therefore a number of operating philosophies, each specific to a plant, have arisen. In almost all concentrators the SAG operation is an evolving operation. Every year, ways and means are sought to increase capacity, decrease energy consumption and prolong lifter and liner life. Newer designs of lifters and redesign of grates and pulp lifters are one of the routes.

The purpose of installing liners in grinding mills is to protect the mill shell from wear and efficiently transfer the energy to the grinding media. The liner profile in the grinding mill determines the energy transfer from the mill shell to the cascading and cataracting charge. However, over the useful lifespan of shell liner, wear leads to change in it's profile, which results in continuous change in the energy transfer to the cascading and cataracting charge. Also, cost of shell liners replacement and the production loss in relining represents a significant amount in the operating cost. Hence, a methodical study of liner wear and its influence on the breakage field is essential for understanding the influence of shell liner wear on mill throughput over the life span of line life.

In the last three decades, significant advances have been made in the modeling of tumbling mills. These investigations led to implementation of the well established techniques like population balance method and discrete element method for design and operation of tumbling mills. The present work details the development and implementation of a shell liner wear model based on Archard's wear law in the discrete element method simulation package *MILLSOFT*. This simulation routine can predict the wear profile of tumbling mill shell liners.

In addition, pilot scale experimental studies were carried out to analyze the effect of liner wear on the product size distribution and residence time distribution. It is shown that liners when slightly worn, after being in operation for about 4 weeks, operate at the highest energy efficiently.

The energy efficiency of these high-throughput grinding mills can be attributed to the field of breakage and slurry transport. The charge motion and breakage of particles inside the mill depends on the shell lifter design, while the discharge of ground particles is controlled by the grate and pulp lifters. The design of these mill components has been largely based on trial and error and hence varies considerably between manufacturers. A study done at the Cortez Gold Mines SAG mill shows how the redesign of the shell lifter brings about a reduction in energy consumption when slurry transport through the mill is adequate.

3. EXPERIMENTAL SETUP

This section covers the experimental set-up, test procedure, industrial mill survey and data collection. The details are provided and discussed under the following two sub-sections:

1. Pilot grinding mill
2. Industrial data collection

3.1 Pilot Grinding Mill Set-up

Experimental studies were conducted on the existing pilot ball-mill set-up shown in Figure 3.1. The pilot ball mill was initially built for studying mass transport on a wet overflow ball-mill. The pilot-scale mill was a 0.416 m diameter by 0.641 m long and 18 mm thick cylindrical steel shell. On the shell there was a rectangular opening of 178 mm by 127 mm through which grinding balls were introduced or removed. The feed end was a steel plate with a 51-mm diameter hole at the center to which a drum feeder is attached. A screw feeder 3 m long and 0.127 m diameter was used to transport ore from the bin to the drum feeder. The existing overflow-discharge end was replaced with a grate plate. The grate plate had five concentric circles with respectively 80, 80, 64, 64 and 48 circular holes of 60 mm diameter. Two roller bearings were installed on the mill frame near the discharge end to support the mill shell.

A torque sensor between the motor and the gearbox measured the torque at the drive side of the gear box and sent its electrical signal to a digital indicator. A triangular mill supported the mill assembly. A Rice Lake™ weighing system, which includes three paramount ™ load sensors anchored to the supporting concrete block. Hence, the triangular frame rests on the load sensors.

The load cell and the torque sensor were calibrated by professionals prior to the test work. To make the mill operation similar to that of a grate discharge mill, a feed water tank and feed water flow system, pump, discharge launder, grate, and pulp lifter were added to the pilot circuit. The 900 L feed water tank was fixed near the mill. Water from the tank was fed to the mill by a Bell & Gosstt pump via two water flowmeters with capacities zero to two L/min and two to 20 gal/min respectively. The output of the pump was connected to the flowmeters. The flow into flowmeters was controlled by the knife-gate valve and the water by-pass system.

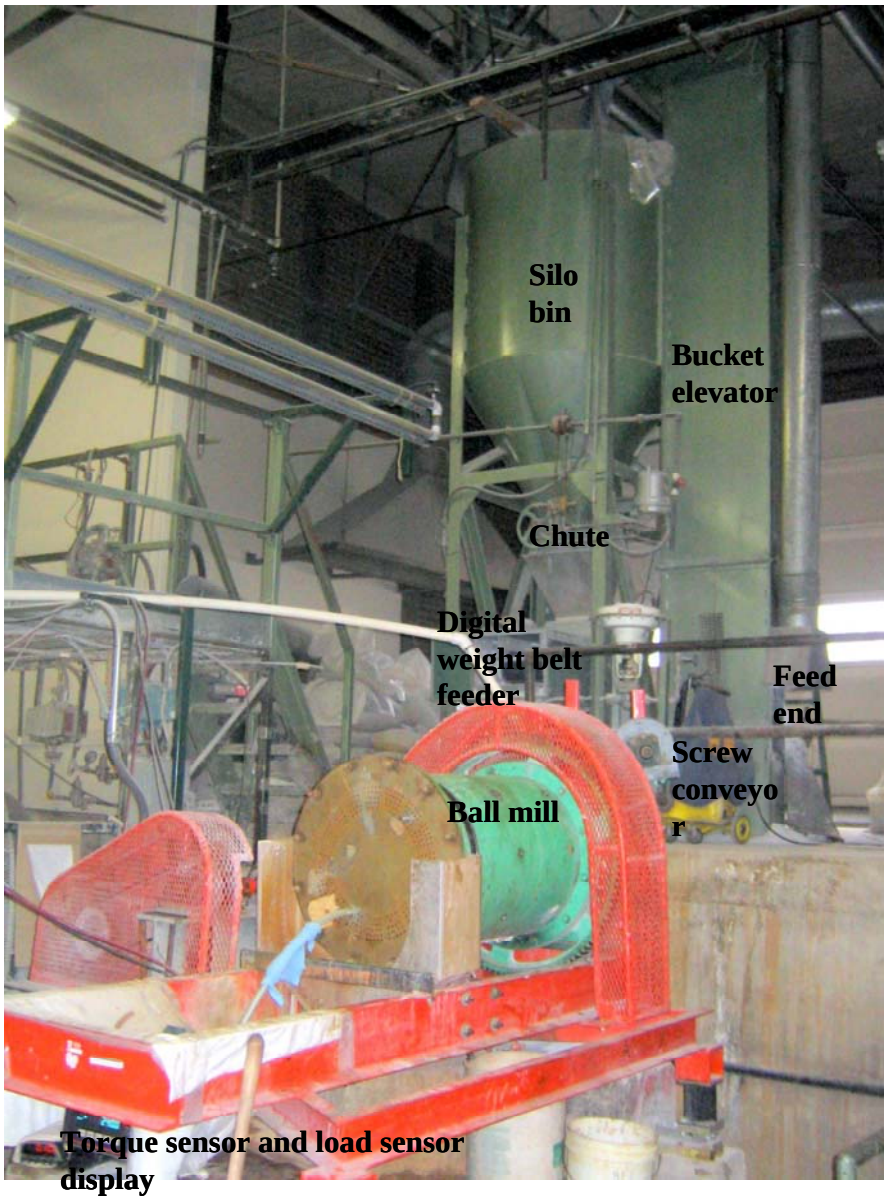

Figure 3.1 Schematic view of the pilot mill

3.1.1 **Discharge Grate and Pulp Lifter**

Discharge grate and pulp lifter assembly was manufactured according to experimental requirements for the pilot-scale mill. The grate plate was manufactured of stainless steel and the pulp lifter is made with Plexiglas^{TM}. Figure 3.2 and Figure show the dimensions of the pulp lifter and grate plate assembly used for experiments. The design variables of the manufactured grate plate, pulp lifter and shell lifter are given in Figure 3.3. Figure 3.4 and Figure 3.5 shows the grate discharge and grate-pulp lifter discharge system installed in the pilot scale ball mill.

3.1.2 **Shell lifter**

Two successive shell lifters lock up the ball mass and raise it to a height, thus working against gravity. The presence of lifters restricts the slippage of charge and enhances the tumbling action of the grinding media.

Three different types of shell lifters were manufactured to study the effect of shell liner wear on the product size distribution. The three liner designs represent liners at three different phases of their life.

Table 3.1 Design variables of different accessories used for investigation in pilot mill

Design Variables	
Shell Lifter	
Face angle	7.5°, 15° and 30°
Height	18, 16 and 12 mm
Grate	
Grate open area (% of mill cross-section area)	6
Number of holes in five circles	80, 80, 64, 64 and 48
Pulp Lifter	
Pulp lifter size(depth)	20 mm
Pulp lifter design	radial
Number of segments	8

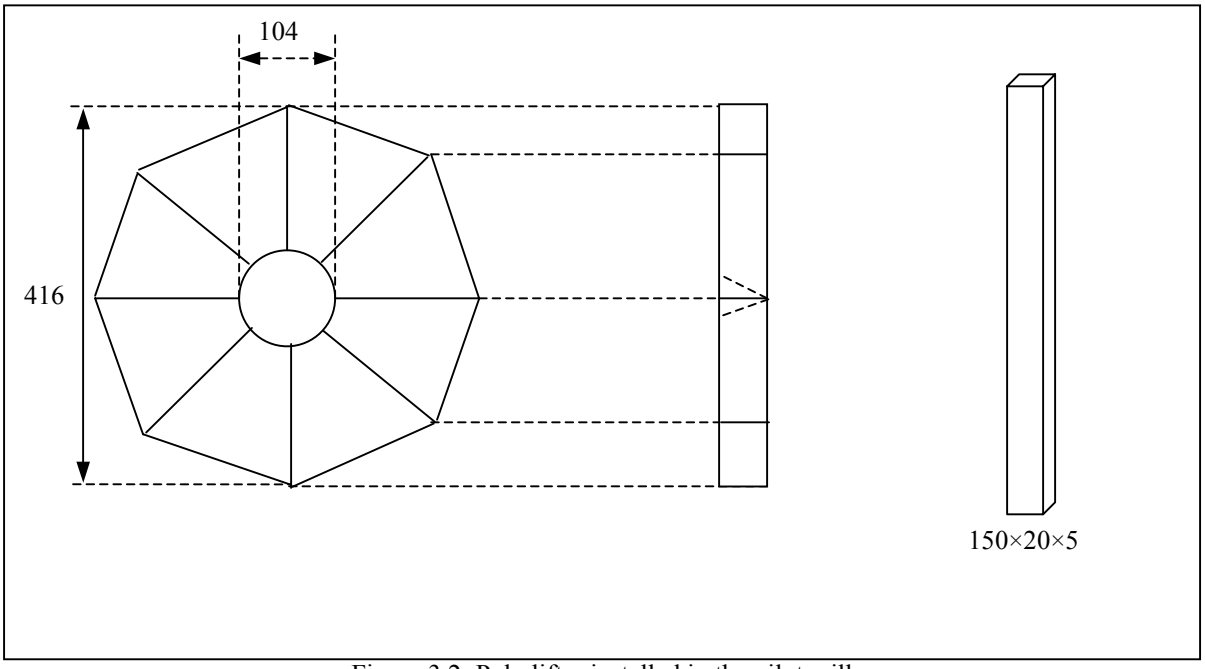

Figure 3.2: Pulp lifter installed in the pilot mill

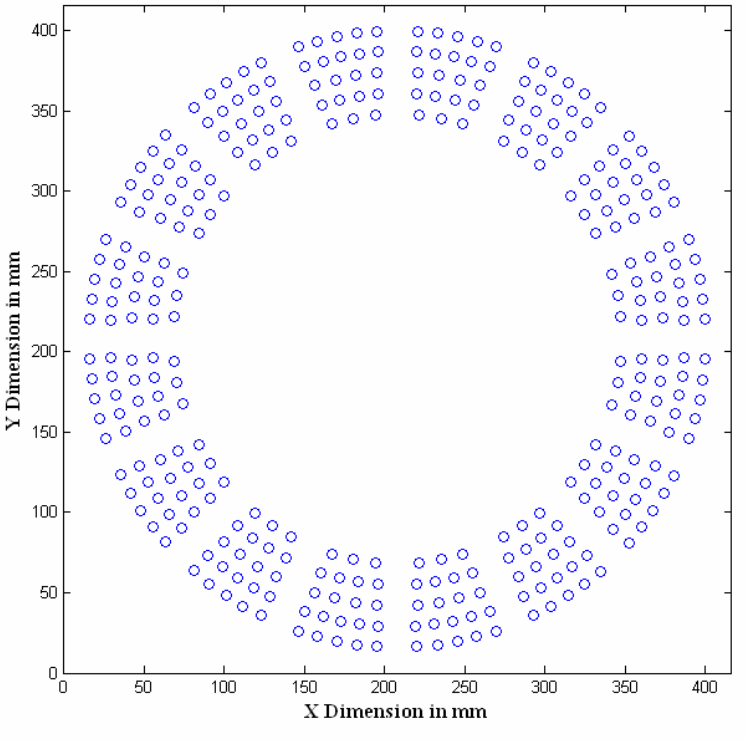

Figure 3.3: Grate plate installed in the pilot mill

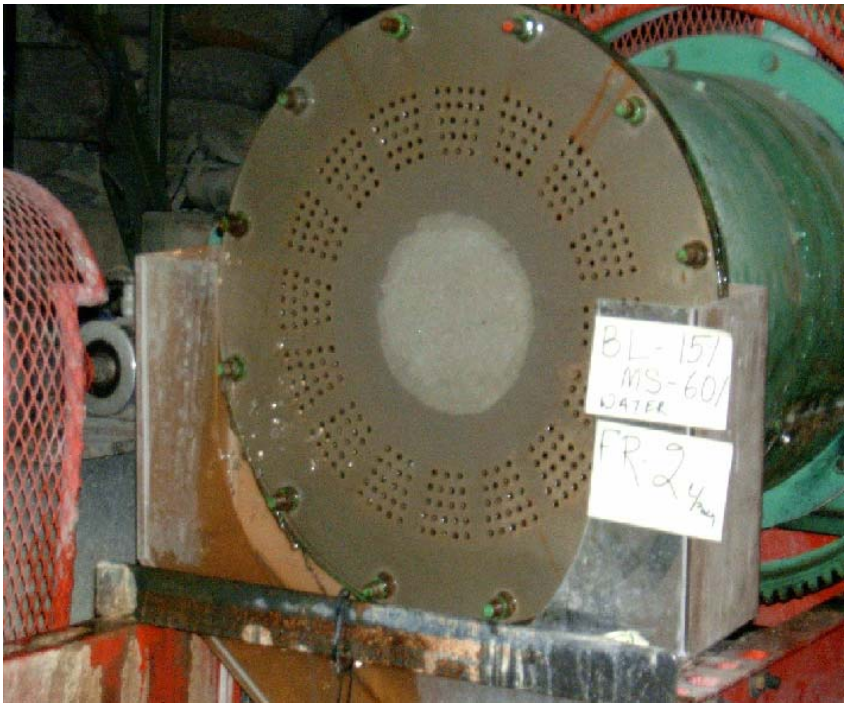

Figure 3.4: Grate plate installed in the pilot scale ball mill

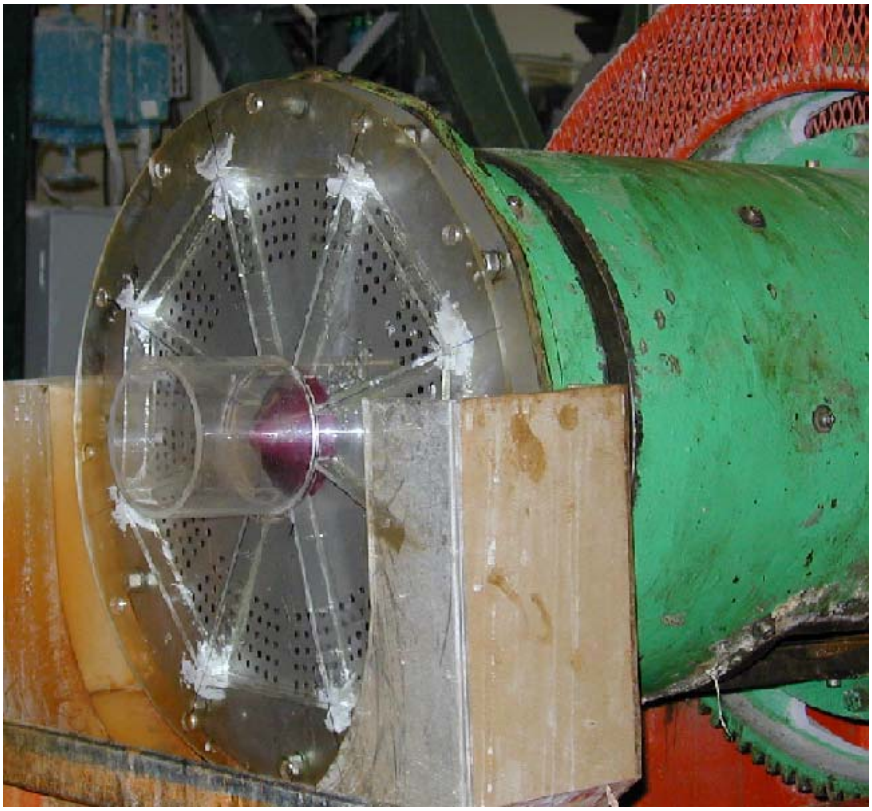

Figure 3.5: Grate and pulp lifter assembly installed in the pilot scale ball mill

For successive liners, the height of the liner was reduced while increasing the face angle to simulate the change in liner profile due to wear. Figure.3.66 and Figure.3. show the front view and top view of the manufactured shell lifters. In Figure.3. the bolt-hole pattern necessary to fix the lifter to the mill shell is also shown. The installed shell type I shell liners are shown pictorially in Figure 3.8.

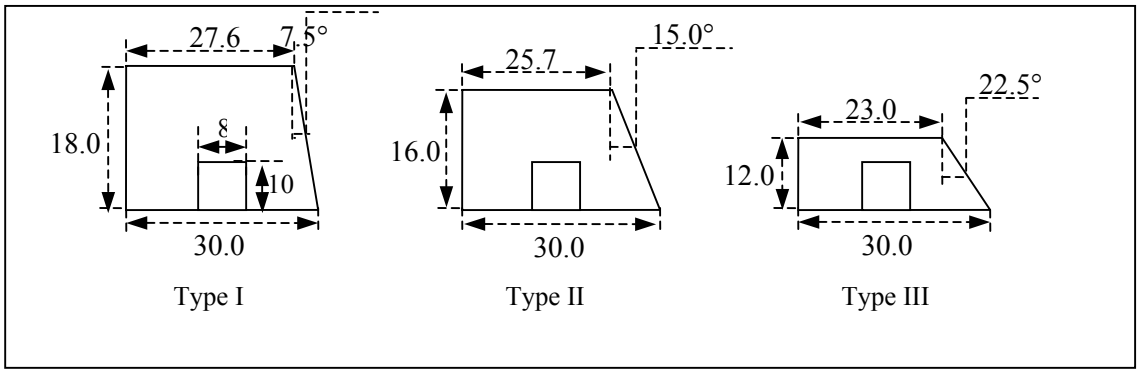

Figure.3.6 Front views of shell lifter profiles (dimensions in mm)

Figure.3. 7 Type I Shell lifter (dimensions in mm)

Figure 3.8 Shell lifters type I installed in the pilot scale ball mill

Table.3.2 Different variables investigated in the pilot mill for experimental studies

Process Variables	
Charge Volume (% of mill volume)	15, 25 and 35
Mill Speed (% of critical speed)	60, 70 and 80
Water flowrate	0.5 to 70 l/min
Solids flowrate	2, 4 , 6 and 10 lb/min

3.1.3 **Test Conditions**

The process variables whose effects were investigated in the pilot-scale mill are listed in the Table 3.2. Tests were conducted at different operating conditions with feed rate ranging from 2 lb/min to 10 lb/min, critical speed ranging from 60% to 80%. Experiments were conducted with both discharge arrangements with grate-only and with grate-pulp lifter. Three different lifter profiles were used for experiments. A list of operating conditions, the lifter design and the discharge type for different test runs is given in Table 3.3.

Table.3:3 Experimental conditions for continuous grinding tests

Test ID	Shell lifter type	Discharge type	Solids Feed Rate (lb/min)	Speed %CS	Residence time distribution	Product size analysis
A-100	Type – I	Grate only	2	70	Yes	Yes
A-101	Type – I	Grate only	4	70	Yes	Yes
A-102	Type – I	Grate only	6	70	Yes	Yes
A-103	Type – I	Grate only	10	70	Yes	Yes
B-100	Type – II	Grate only	2	70	Yes	Yes
B-101	Type – II	Grate only	4	70	Yes	Yes
B-102	Type – II	Grate only	6	70	Yes	Yes
B-103	Type – II	Grate only	10	70	Yes	Yes
C-100	Type – III	Grate only	2	70	Yes	Yes
C-101	Type – III	Grate only	4	70	Yes	Yes
C-102	Type – III	Grate only	6	70	Yes	Yes
C-103	Type – III	Grate only	10	70	Yes	Yes
C-104	Type – III	Grate only	4	60	No	Yes
C-105	Type – III	Grate only	4	80	No	Yes
C-106	Type – III	Grate only	10	60	No	Yes
C-107	Type – III	Grate only	10	80	No	Yes
D-100	Type – III	Grate – pulp lifter	4	60	Yes	Yes
D-101	Type – III	Grate – pulp lifter	4	70	Yes	Yes
D-102	Type – III	Grate – pulp lifter	4	80	Yes	Yes
D-103	Type – III	Grate – pulp lifter	10	60	No	Yes
D-104	Type – III	Grate – pulp lifter	10	70	No	Yes
D-105	Type – III	Grate – pulp lifter	10	80	No	Yes

3.1.4 **Pilot mill experiment procedure**

After calibrating the solids feed system, water feed system, torque sensor, and load sensor, the pilot mill was used with the following simple experimental procedures. A simple water-only experiment for measuring hold-up was carried out as follows.

1. Initial inspection was carried out on all the equipment for any loose parts or anything that could lead to circuit failure.
2. The speed controller was set to the desired mill speed.
3. The flow rate of water was calculated so as to give the desired water flow rate.
4. The percent ball load in the mill was rechecked, and the initial reading on the load sensor was recorded. The water system was checked for any leakage. The pump was switched on.
5. The reading on the load sensor was recorded every two minutes.
6. Steady-state condition was achieved once the weight indicator display did not show an increasing or decreasing trend.
7. The final reading on the weight indicator was recorded and the water hold-up in the mill was calculated by subtracting the no-load hold-up mass.

The experimental procedure for measuring hold up and sampling the mill product was carried out as follows:

1. Initial inspection was carried out on all the equipment for any loose parts or anything that could lead to failure of the circuit.
2. The stock of solids in the silo was checked and refilled if necessary.
3. The speed controller was set to the desired mill speed.
4. The flow rates of water and solids were calculated so as to give a desired slurry flow rate.
5. The percent ball load in the mill was rechecked, and the initial reading on the load sensor was recorded.
6. The water system was checked for any leakage. The motor was switched on, and, simultaneously, the solids feed system was switched on.
7. The reading on the load sensor was recorded every two minutes.

8. Steady-state condition was achieved once the weight indicator display did not show an increasing or decreasing trend.
9. The final reading on the weight indicator was recorded and the slurry hold up in the mill was calculated by subtracting the no-load hold up value.
10. After steady state was achieved, the mill was in operation for about half an hour.
11. One or two timed samples were collected at the discharge launder of the mill.
12. The percent solids of the product timed-sample slurry were calculated and cross-checked with that of the feed slurry.
13. Wet screening of the sample on a 100-mesh sieve was carried out. The plus 100-mesh sample and minus 100-mesh sample were kept for further sieve analysis.
14. Both of the slurry samples were weighed, filtered, and dried for size analysis.
15. Coning and quartering of the minus 100-mesh fraction sample was carried out and a 400- to 500- gm sample was set aside for carrying out sieve analysis.
16. The final size analysis of the product was obtained by combining the size analysis of the minus 100-mesh and plus 100-mesh fractions.
17. Duplicate samples of the discharge product taken periodically were analyzed for particle size distribution and slurry percent solids.

3.1.5 **Procedure for residence time distribution (RTD) experiment on the pilot mill**

Lithium Chloride was used as a tracer material for performing residence time distribution studies. The inductive coupled plasma (ICP) analyzer available at the University of Utah (406, Browning building) was calibrated for lithium concentrations 10,000 ppm. So the quantity of lithium chloride to be added in the circuit was in the detectable range of concentration. A maximum concentration of 1000 ppm (1 gram per liter of slurry) was judged to be a good number to use for the high flowrates.

- Typically 5 grams of lithium chloride as tracer element was used in all the experiments.
- The tracer material was dissolved in the water and was injected in the feed water stream near the feed end of the mill.
- The times of tracer injection and sample collection were synchronized.

- The total duration of sample collection was judged to be at least three times the retention time.
- Samples were collected at a time interval of 15 sec to 1 min depending on mill feed rate. The appendix gives detailed information about the time intervals used to collect samples.
- One or two samples were collected before the tracer was added to estimate the background lithium concentration in the slurry.
- Once the samples were collected and filtered, the filtrate was stored in 100-ml bottles which were sealed with proper labeling.

4 RESULTS AND DISCUSSION

4.1 Continuous grinding tests

Grinding tests were carried out to analyze the effect of different process and design variables on the product size distribution of the mill. One of the main investigations in this thesis work is to evaluate the effect of liner wear on the breakage field of the grinding process. Different liner were manufactured and installed in the grinding mill for facilitating the experimental work. Experiments were carried out to investigate

- The effect of solids feed rate on the product size distribution and residence time distribution.
- The effect liner profile on the product size distribution and residence time distribution.
- The effect of mill speed on the product size distribution and residence time distribution.
- The effect of discharge type (grate only, grate-pulp lifter) on the product size and residence time distribution.

4.1.1 Product size analysis studies

The breakage field in the grinding mill is reflected directly on the fineness of the product. If the efficiency of the grinding is higher, generally the product becomes finer. Alternatively, a poor breakage field inside the mill yields a coarse product and hence less grinding. A series of experiments were designed to study the effect of different design and process variables on the product size of the mill.

4.1.1.1 Effect of solids feed rate

The solids feed rate to the mill has significant impact on the output product size. Usually, in concentrators, the grinding mill operates at a stipulated feed rate. The feed rate is fixed at the design stage. A minor variation in the feed rate changes the fineness in the product size of the mill. So, better understanding of the effect of feed rate on the product size could result in better efficient grinding.

The pilot-scale mill was run at four different feed rates viz. 2, 4, 6 and 10 lb/min. The solids percentage in the slurry was maintained at 69.4% in all of the experiments. The water flow rate to the circuit was determined accordingly. Experiments with different feed rates were repeated with all the three different liners. Each liner was installed in the mill and experiments at 2, 4, 6 and 10 lb/min solids feed rate were carried out. The product samples were collected and processed to get the product size distribution. The product size distribution for different solids feed rates is compared in Figure 4.1. The experiments were carried out with shell liner type I installed in the mill. Similarly, all the experiments were carried out with shell liner type II and type III in the mill. Figure 4.2 and Figure 4.3 show the respective product size comparison graphs for experiments with type II and type III shell liners. The Figures 4.1- 4.3 shows that as the solids feed rate increases the product becomes finer which can be attributed to the decrease in mean residence time of the charge. The mean residence time comparison studies are illustrated in a later section of this chapter.

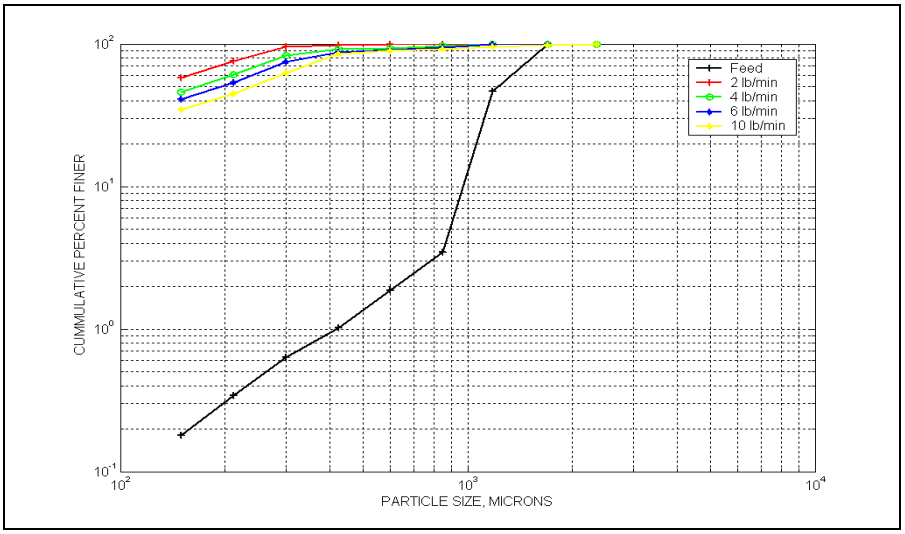

Figure.4.1 Size analysis of the mill feed and discharge (25% ball load, 69.4% solids, 70% of critical speed, type-I shell, grate-only) at different feed rates varying from 2 to 10 lb/min

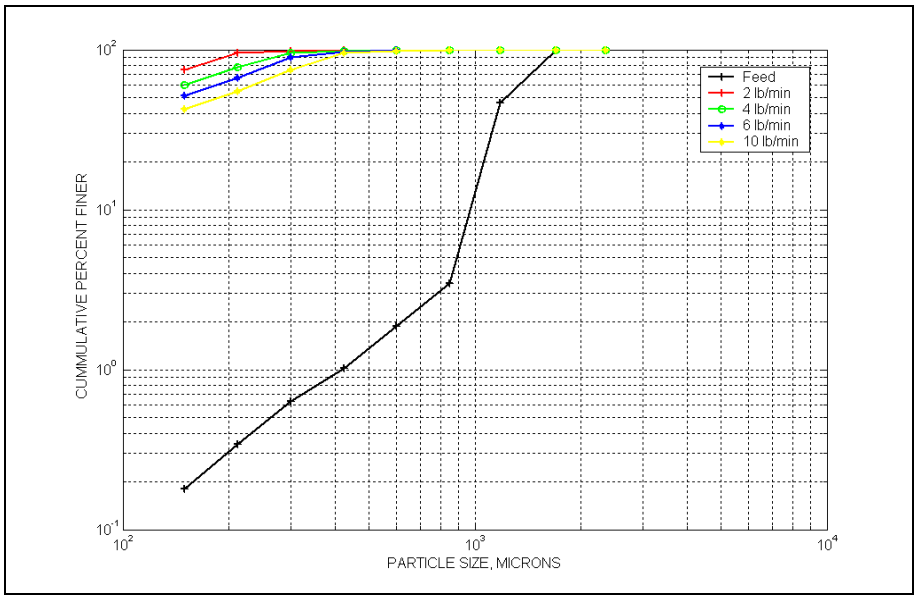

Figure.4.2 Size analysis of the mill feed and discharge (25% ball load, 69.4% solids, 70% of critical speed, type-II shell, grate-only) at different feed rates varying from 2 to 10 lb/min

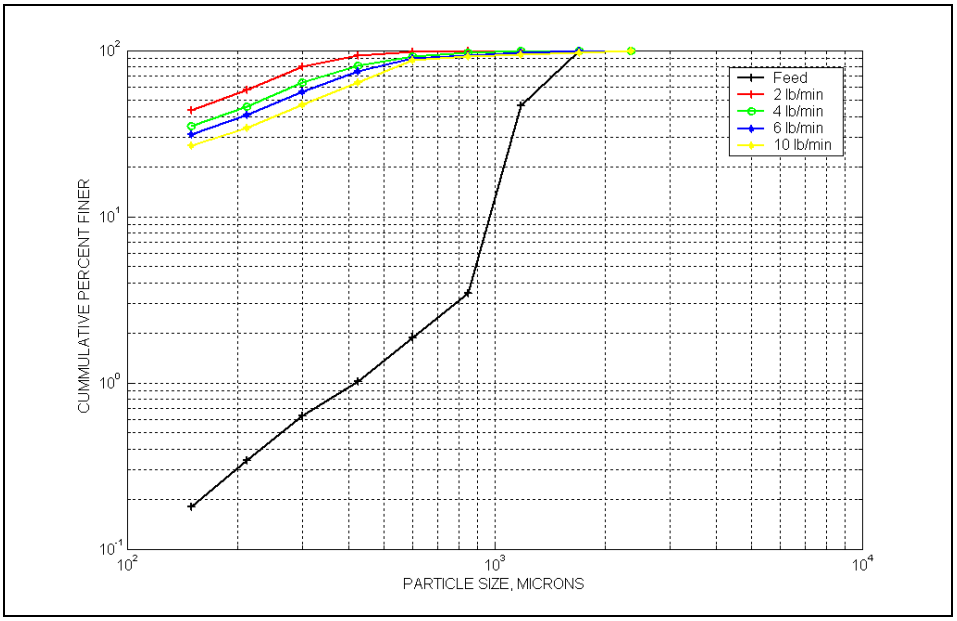

Figure.4.3 Size analysis of the mill feed and discharge (25% ball load, 69.4% solids, 70% of critical speed, type-III shell, grate-only) at different feed rates varying from 2 to 10 lb/min

4.1.1.2 Effect of shell liner profile

The life of steel shell liner for any industrial SAG mill operation is between 4 to 8 months. The replacement of the shell liner is expensive in-terms of replacement cost and downtime loss. Hence, the present work extensively deals in understanding the liner wear and its effect on the breakage field in grinding mills.

The wearing of liner leads to change in its profile. Hence, the wearing of the liner changes the extent of charge lift, the cascading and cataracting grinding zones. In general, it causes overall change in breakage field in the grinding process. Hence, in this study an attempt was made to understand the effect of liner wear on the product size distribution and residence time distribution.

The three types of the liner profile configurations were show in Figure 5.4. Each type of shell liner was installed in the pilot-scale mill and experiments were carried out at 2, 4, 6 and 10 lb/min solids feed rate. The detailed experimental condition and the results are given in the Appendix. The relevant experiments to this study are A100-A103, B100-B103 and C100-C103.

The product size distribution at 2 lb/min solids feed rate for different liner profiles are compared in Figure 4.4. From the Figure 4.4, it can be observed that, the product size for the experiment with type II shell liner is finer then for type I and type III shell liner. Also, type III liner experiment produces the coarsest product size amongst the three liners. Hence, the grinding efficiency of the mill is better when type II liner was installed than type I and type III liners. With type II liner, the charge experiences optimized motion (both cataracting and cascading), yielding in finer product size for type I shell liner. For type III liner, the face angle is so low that, the charge could hardly be lifted for any impact grinding. Similar phenomena were observed in experiments with all other feed rates viz. 2, 4, 6 and 10 lb/min solids feed rate. Figure 4.5 to Figure 4.7 compares the product size distribution at different feed rates viz. 2, 4, 6 and 10 lb/min respectively for different liner profiles. The trend observed for feed rates 2 lb/min is also observed with feed rates at 4, 6 and 10 lb/min.

4.1.1.3 Effect of mill speed with grate-only discharge type

Mill speed has significant impact on the product size. Experiments were carried out at 60, 70 and 80 percent critical speed of the mill for 4 and 10 lb/min solids feed rate, to observe the effect of mill speed on the product size distribution. The relevant experiment data sets are C101, C104, C105, C103, C107 and C108.

Figure 4.8 shows the comparison plot of product size distribution for the experiments at 60, 70 and 80 percent critical speed at 4 lb/min solids feed rate. With increasing speed from 60 to 80 percent critical the

product gets finer. Similarly, Figure 4.9 shows the corresponding comparison chart for experiments at 10 lb/min solids feed rate. A similar trend is observed in the experiments with 10 lb/min solids feed rate.

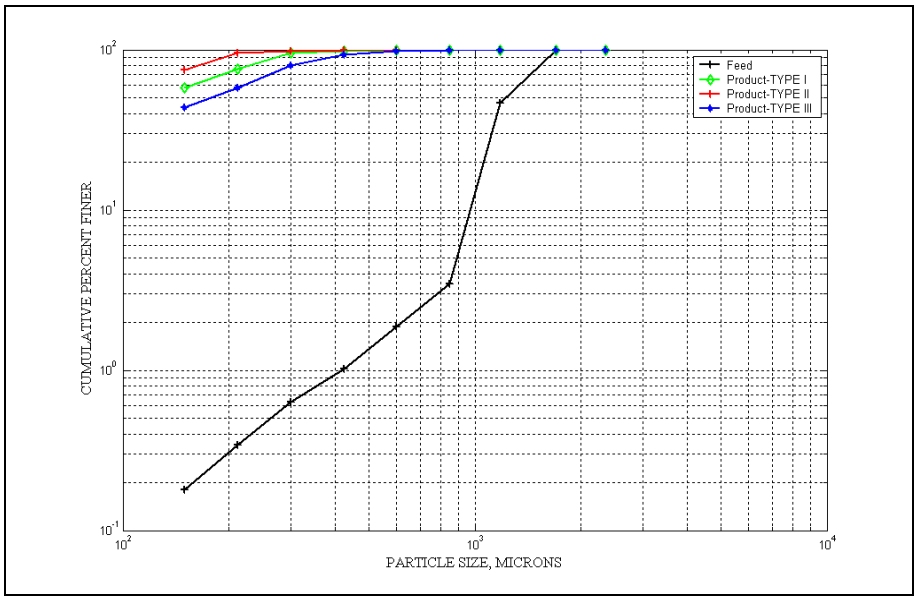

Figure.4.4 Size analysis of the mill feed and product (25% ball load, 69.4% solids, 70% of critical speed, 2 lb/min feed rate, grate-only) for different types of shell liners

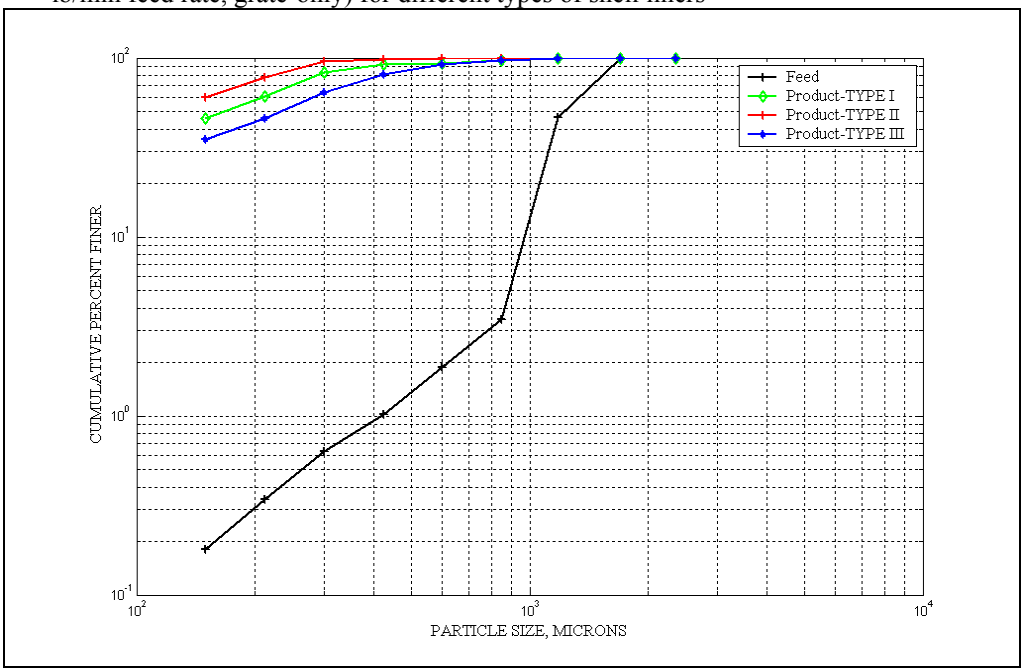

Figure.4.5 Size analysis of the mill feed and product (25% ball load, 69.4% solids, 70% of critical speed, 4 lb/min feed rate, grate-only) for different types of shell liners

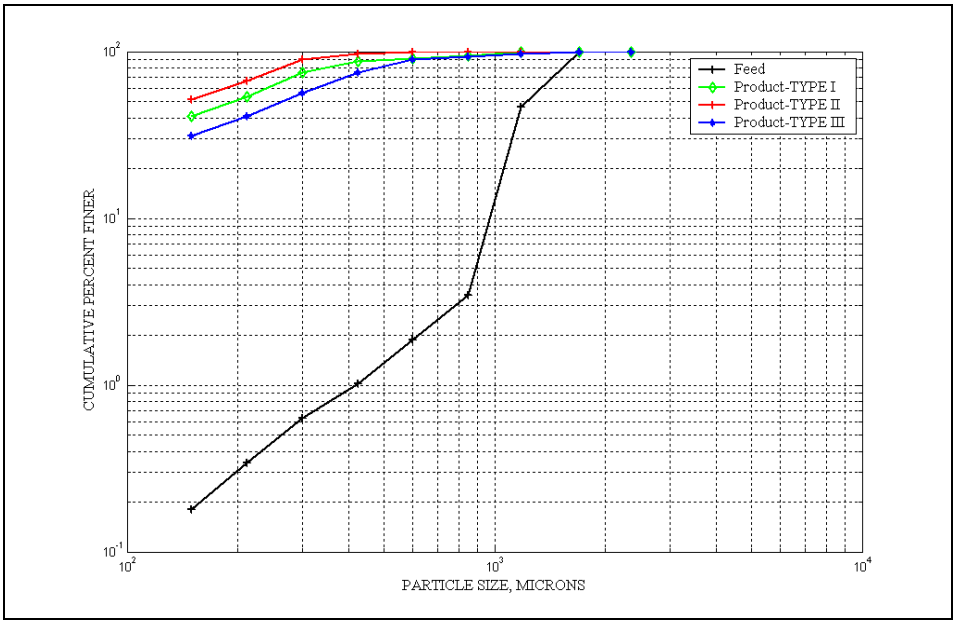

Figure.4.6 Size analysis of the mill feed and product (25% ball load, 69.4% solids, 70% of critical speed, 6 lb/min feed rate, grate-only) for different types of shell liners

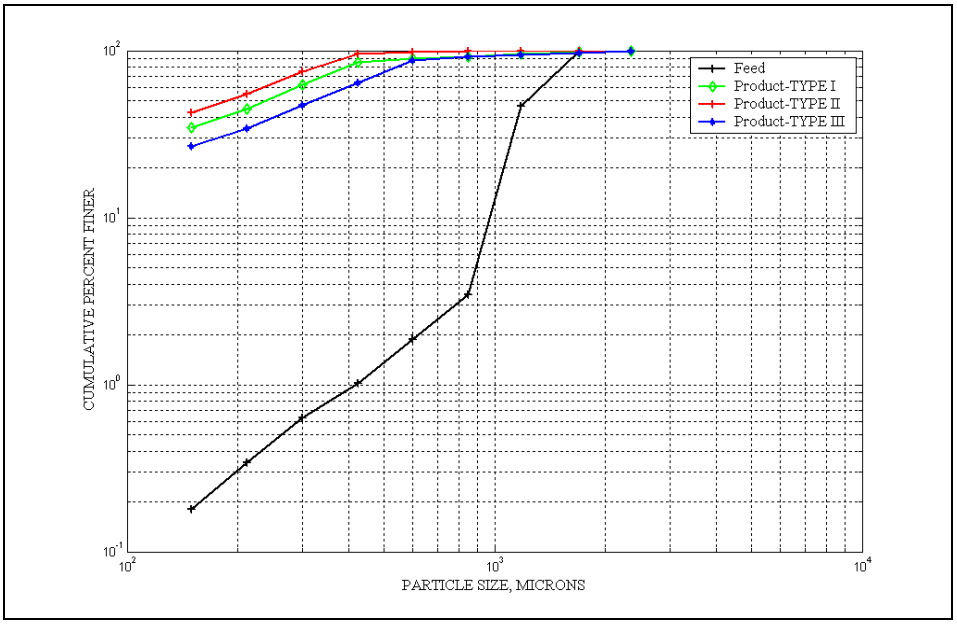

Figure.4.7 Size analysis of the mill feed and product (25% ball load, 69.4% solids, 70% of critical speed, 10 lb/min feed rate, grate-only) for different types of shell liners.

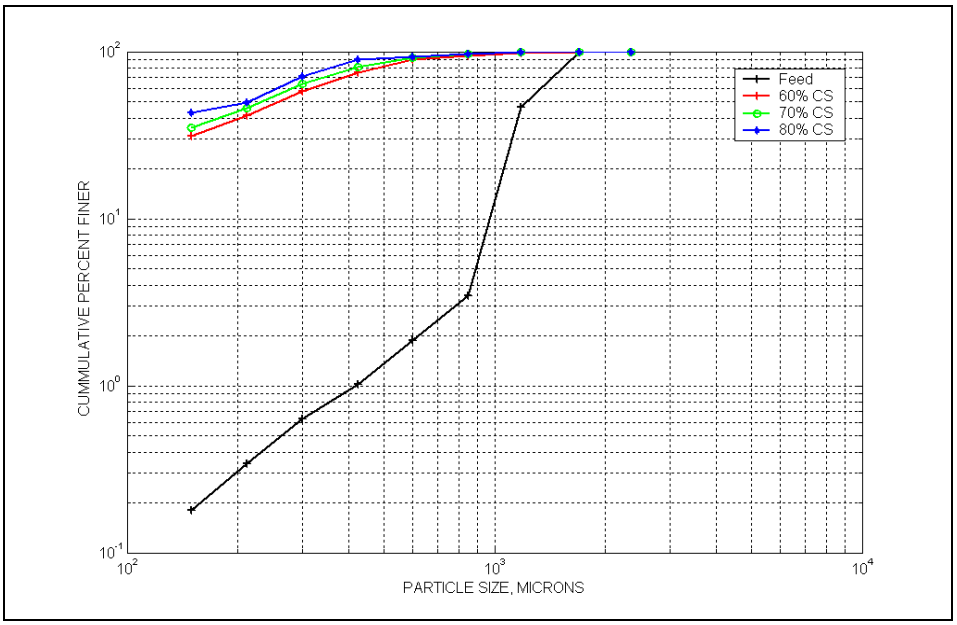

Figure.4.8 Size analysis of the mill feed and product (25% ball load, 69.4% solids, 4 lb/min feed rate, shell liner type-III, grate-only) for different mill speed

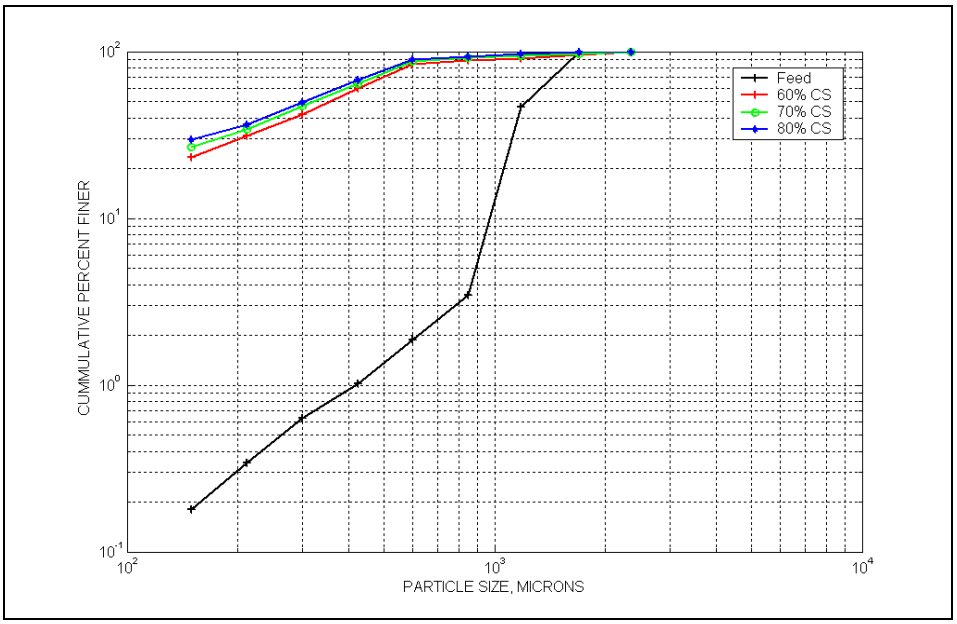

Figure.4.9 Size analysis of the mill feed and product (25% ball load, 69.4% solids, 10 lb/min feed rate, shell liner type-III, grate-only) for different mill speed

4.1.2 Residence time distribution studies

Residence time distribution is an important grinding operation parameter. Residence time distribution and mean residence time strongly depend on the process variables viz. feed rate, mill speed, shell liner and pulp lifter design. In this study an attempt is made to analyze the effect of the above process and design variables on the residence time distribution of the grinding process.

4.1.2.1 Effect of solids feed rate

The solids feed rate to the mill has significant impact on the residence time distribution and mean residence time. The simple correlation between mean residence time and feed rate is shown in Equation 6.1

$$\tau = \frac{Holdup}{Flowrate}. \qquad (6.1)$$

Experiments were carried out at 2, 4, 6 and 10 lb/min solids feed rate. The pertinent experiments are given in Table 4.1. The experiments were repeated after installing type-I, type-II and type-III shell liners. Figure 4.10 shows the comparison plot of residence time distribution obtained from tracer concentration data collected for experiments at 2, 4, 6 and 10 lb/min solids feed rate. The above experiments were carried out with type-I liner installed in the mill. Similarly, experiments were carried out with type-II and type-III liners installed are also shown in Figure 4.11 and Figure 4.12. In all the above comparison plots, as the feed rate increases the τ of the charge decreases. For example with 2 lb/min solids feed rate and type I liner installed, the τ is 5.43 min where as with 10lb/min solids feed rate at similar conditions the τ is 2.62 min. Also, as the feed rate to the mill increases the peak concentration of the exit tracer decreases. This trend is observed in the experiments with different feed rates.

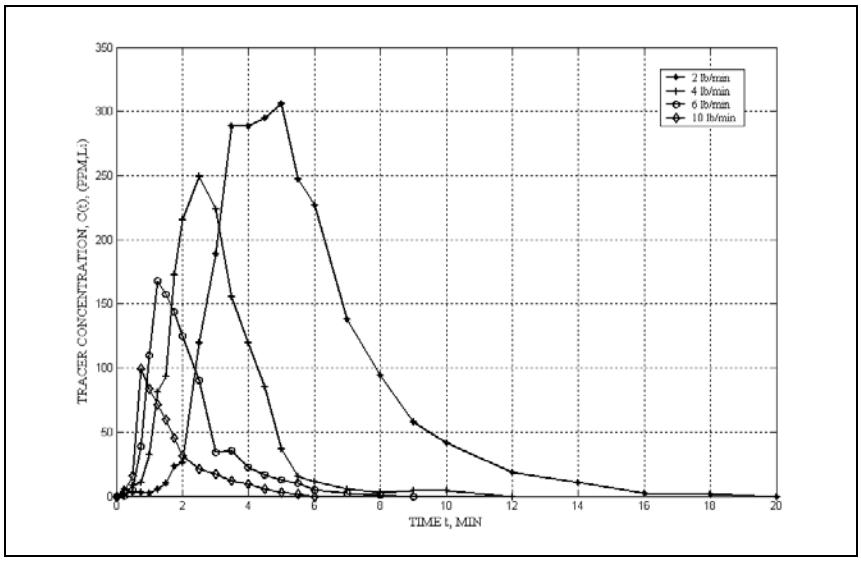

Figure.4.10 Experimental residence time distribution of the mill discharge product (25% ball load, 69.4% solids, shell liner type-I, grate-only, 70% of the critical speed) for different feed rates

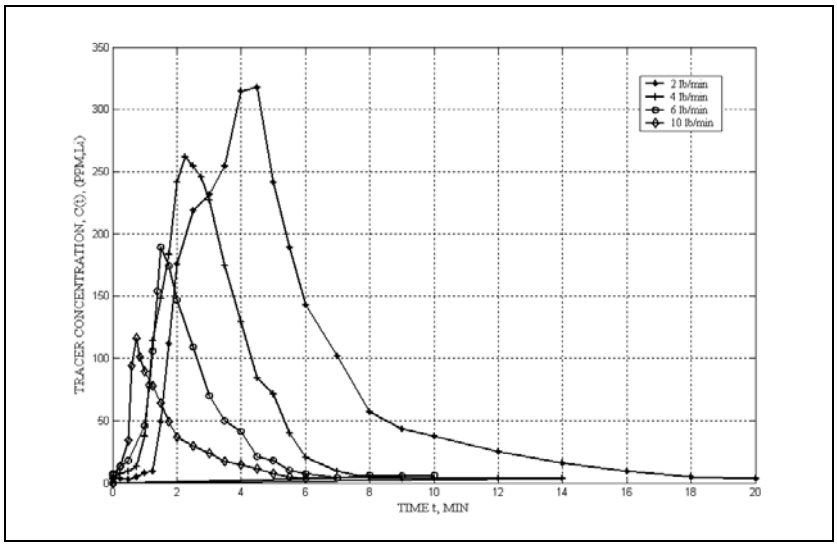

Figure.4.11 Experimental residence time distribution of the mill discharge product (25% ball load, 69.4% solids, shell liner type-II, grate-only, 70% of the critical speed) for different feed rates

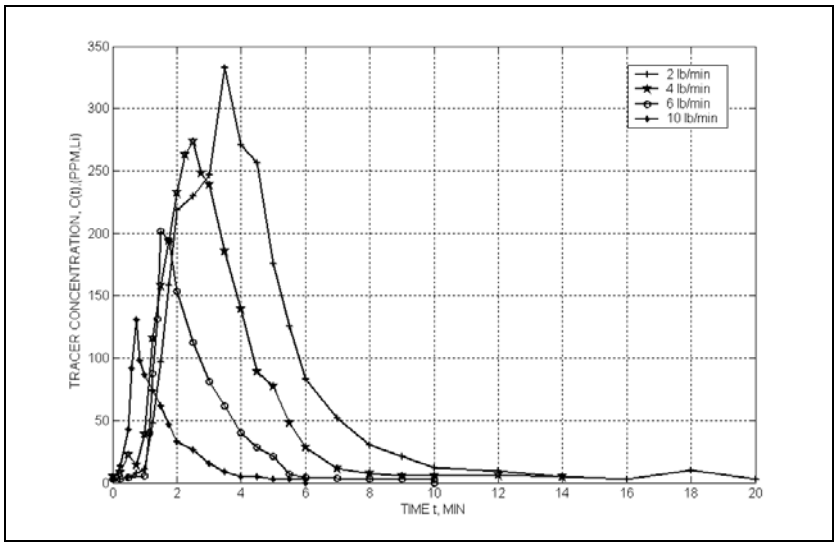

Figure.4.12 Experimental residence time distribution of the mill discharge product (25% ball load, 69.4% solids, shell liner type-III, grate-only, 70% of the critical speed) for different feed rates

Table 4.1 List of experiments lists effect of solids feed rate on residence time distribution

Figure Number	Experiment Number
Figure 4.10	A100 to A103
Figure 4.11	B100 to A103
Figure 4.12	C100 to C103

4.1.2.2 Effect of shell liner

The effect of shell liner wear on the τ was examined. The experimental mean residence times for all the experiments carried out with type-I, type-II and type-III shell liners were calculated from Equation 6.1 and are shown in Table 4.2. The hold-up data were recorded from load sensor display.

Table 4.2 Experimental τ values for different experiments

	Solids feed rate in lb/min			
Shell liner type	2	4	6	10
Type I	5.43	3.57	3.12	2.62
Type II	5.08	3.35	2.90	2.56
Type III	4.43	3.00	2.56	2.44

Table 4.2 shows that at a certain feed rate, the τ value decreases as the shell liner profiles changes from type-I to type-III. This drift of τ from higher to lower values can be noticed at all feed rates viz. 2, 4, 6 and 10 lb/min.

As the liner wears out the cataracting zone in the grinding mill shrinks. This is because of the inability of the worn liner with high face angle to lift charge to a greater extent. The shrink in cataracting zone in-turn reduces the charge hold-up in the mill and also decreases the discharge rate of finer ground particles through grate plate. Figure 4.13 to Figure 4.16 shows the comparison plots of residence time distribution for different shell liners at feed rates 2, 4, 6 and 10 lb/min respectively. The pertinent experiments to this above study are A100 to A103, B100 to B103 and C100 to C103.

4.1.2.3 Effect of discharge type

It has been established by Sanjeeva Latchireddi and Raj Rajamani that an improper design and selection of pulp lifter for industrial SAG mills could result in slurry pool and consequently poor grinding. This is mainly because of the flow-back phenomena explained in the earlier section 6.2.1.4. Although, it is practically impossible to eliminate flow-back because of design limitations, it is possible to reduce it to such an extent so as to get maximum grinding efficiency. Because of the installed pulp-lifter, slurry often gets transported back to the cylindrical shell through the grate plate. Hence, the τ of the charge increases. The above flow-back phenomenon was also observed after conducting and analyzing experiment results on the pilot-scale ball mill. The experiments results are shown in Figure 4.17, which compares the residence time distribution for grate-only and grate-pulp lifter discharge system. It can be seen that, the mean residence time with grate-pulp lifter assembly is 3.71 which is higher than the τ value of 3.0 obtained with grate-only discharge system experiment. The corresponding experiments numbers are C101 and D101.

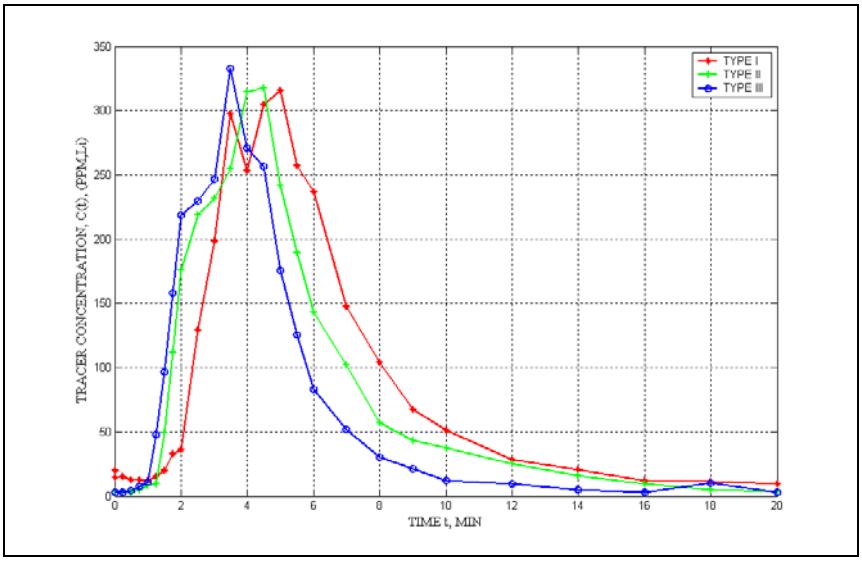

Figure.4.13 Experimental residence time distribution of the mill product (25% ball load, 69.4% solids, grate-only, 70% of the critical speed, 2 lb/min feed rate) for different types of shell liners

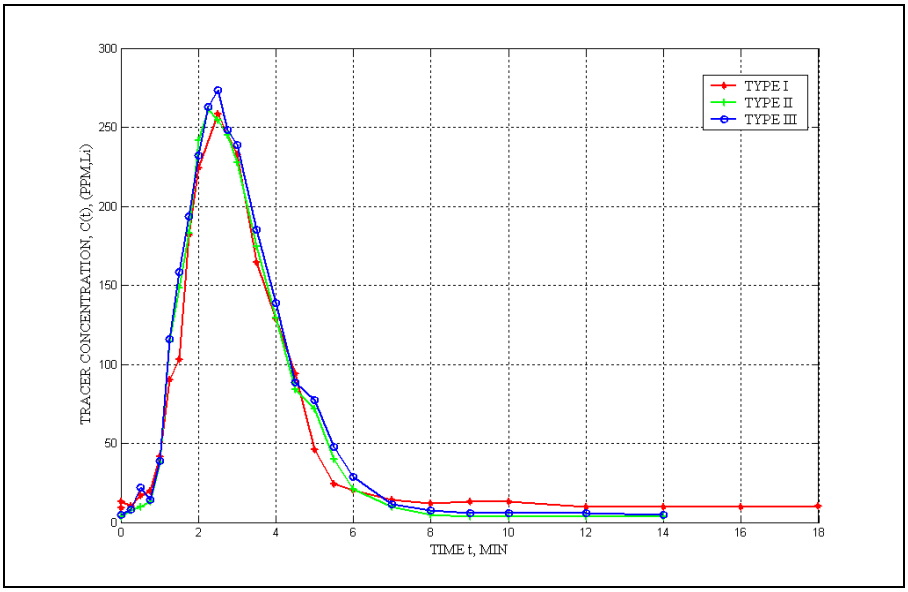

Figure.4.14 Experimental residence time distribution of the mill product (25% ball load, 69.4% solids, grate-only, 70% of the critical speed, 4 lb/min feed rate) for different types of shell liners

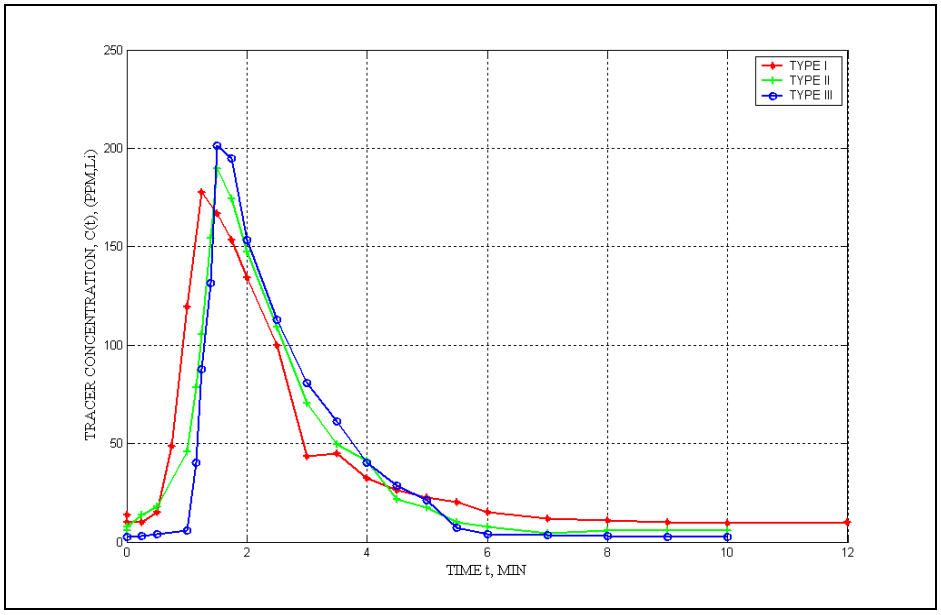

Figure.4.15 Experimental residence time distribution of the mill product (25% ball load, 69.4% solids, grate-only, 70% of the critical speed, 6 lb/min feed rate) for different types of shell liners

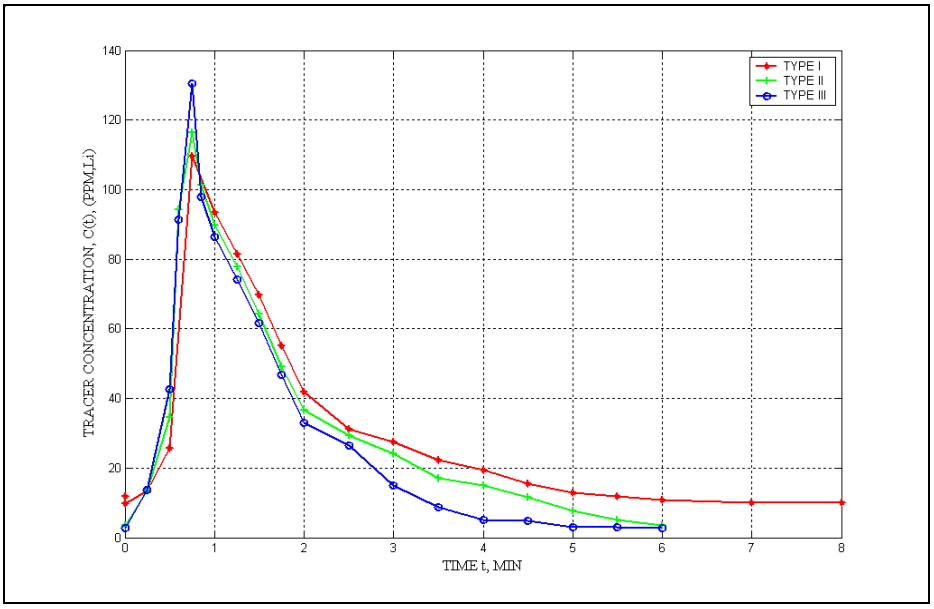

Figure.4.16 Experimental residence time distribution of the mill product (25% ball load, 69.4% solids, grate-only, 70% of the critical speed, 10 lb/min feed rate) for different types of shell liners

The values of j and τ of the experiments with different discharge systems is shown in Table 6.8. With grate only discharge system the flow is less mixed than grate pulp lifter discharge system. This is because of the

flow back of slurry with grate-pulp lifter discharge system. Also due to flow back, with grate pulp lifter discharge system the mean residence time of the slurry increases.

Table 4.3 Comparison of j and τ at 25 different discharge systems

Discharge system	Mean residence time (τ)	Number of mixers (j)
Grate only	3.08	3.94
Grate pulp lifter	3.71	3.91

4.1.2.4 Effect of mill speed

The effect of mill speed on the residence time distribution was analyzed for the grate-pulp lifter discharge assembly pilot-scale ball mill. Figure 4.18 shows the comparison graph of residence time distribution for the experiments at 60%, 70% and 80% critical speed of mill. The τ increases as the mill speed increases from 60% critical speed to 80% critical speed.

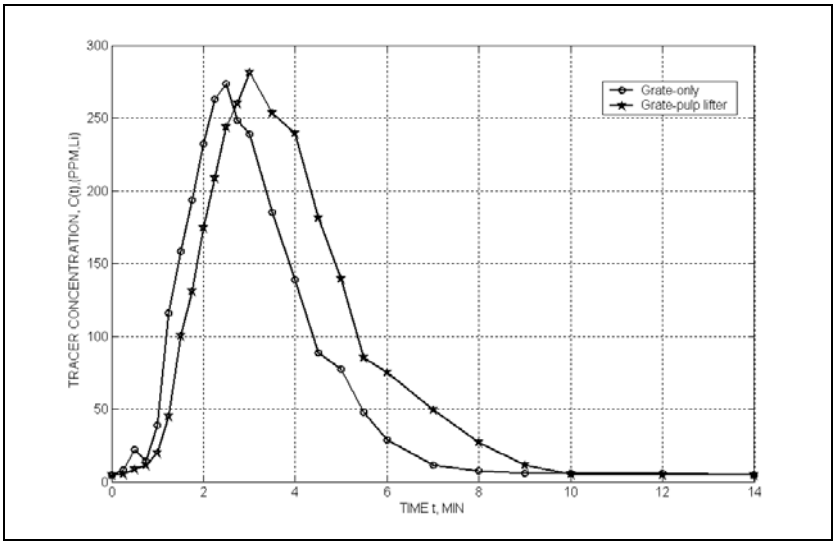

Figure.4.17 Experimental Residence time distribution of the mill product (25% ball load, 69.4% solids, 4 lb/min feed rate, shell liner type-III, mill speed at 70% of the critical speed) for different discharge systems

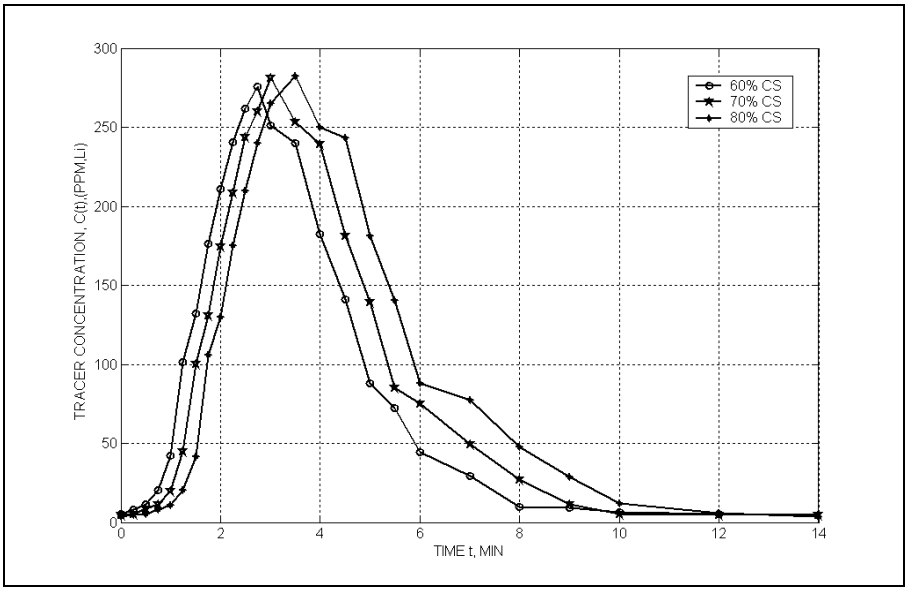

Figure.4.18 Experimental residence time distribution of the mill discharge product (25% ball load, 69.4% solids, 4 lb/min feed rate, shell liner type-III, grate-pulp lifter discharge system) for different mill speed

The number of mixers for all the three experiments remains almost the same. The corresponding experiment numbers are D100, D101 and D102.

4.1.3 **Specific selection function estimation**

The alternate form of selection function, termed specific selection function, arises from energy normalized form of the grinding equation. The specific selection function can be calculated from S_i, as shown in Equation 6.2.

$$S_i^E(Tons/KWH) = S_i(Hours^{-1})H(Tons)/P(KW) \qquad (6.2)$$

This form is selection function is used when specific energy rather than grind times is used for simulation or estimation.

The estimated breakage function values given in Appendix B-1, number of mixers, specific energy, feed and product size distribution data each experiment was input to the ESTIMILL program for evaluating specific selection function. Specific selection function estimation was carried out for A101, B101 and C101 experiments. Figure 4.19 shows the comparison plot of specific selection functions for the experiments A101, B101 and C101. The experiment with type-II liners exhibits higher selection function values than type-III liners. Experiment with

type-I liners give the lowest selection function values. According to the plot, type-II liner is efficient than type-III and type-III liner is efficient then type-I. For this particular study, it can be said that the grinding efficiency in the mid-life phase is better than in initial phase and final phase. These phenomena might not be true in every grinding case. More experiments with very high face angle liner (more than 30°) should be carried out to observe the trend of change in specific selection function with the wearing of liners.

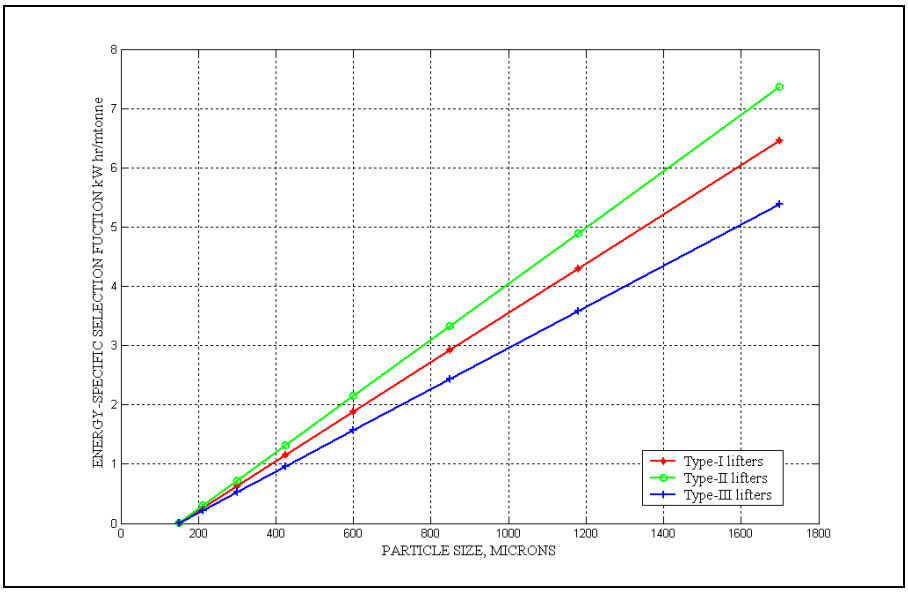

Figure.4.19 Simulated specific selection functions of the mill (25% ball load, 69.4% solids, grate-only, 70% of the critical speed, 4 lb/min feed rate) for different types of shell liners

Specific selection function was estimated for the experiment with grate-pulp lifter discharge type and solids feed rate at 4 lb/min. The obtained specific selection function values were compared with the specific selection function values estimated for the experiment with grate-only discharge system. Except the discharge system, all the other operating and design parameter were kept same for both of the experiments to observe the effect of pulp lifter on the grinding. The specific selection comparison plot is shown in Figure 4.20. According to the graph, the specific selection function values obtained from the grate-pulp lifter discharge system are higher than specific selection function values obtained from grate-only discharge system. Hence, it is concluded that efficient grinding was observed with the grate-pulp lifter discharge assembly than the grate-only discharge assembly.

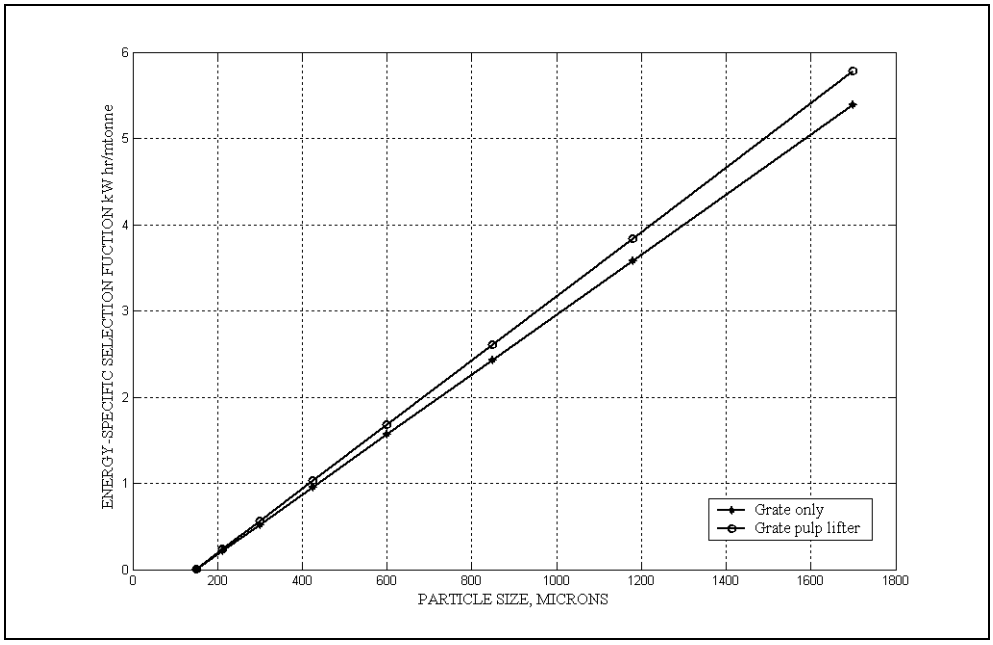

Figure.4.20 Simulated specific selection function of the mill experiments (25% ball load, 69.4% solids, 4 lb/min feed rate, shell liner type-III, 70% of the critical speed) for different discharge systems

5. CONCLUSIONS

Experimental studies were conducted to investigate the effect of liner wear on the product size and residence time distribution in tumbling mills. Three different liner sets representing three phases of the wear life was used in these test. The highest breakage field was observed at the mid-life lifter phase. The rate of breakage was the highest in this phase of lifter life. The product was coarser with mid phase liner profile compared to the initial and final phase lifter profiles. Also, product size analysis of the experiments at different feed rate show that as the feed rate increases the product size becomes finer.

Residence time measurements and direct on-line load measurement showed that hold-up of solids in the mill decreases as the shell liner wears more and more. Experiments at different critical speeds prove that as the mill speed increases from 60% to 80% critical speed, the mean residence time of the charge increases.

Experimental studies were also conducted to observe the effect of pulp lifter on the breakage field in tumbling mill. It was observed that, the grate-pulp lifter discharge assembly produces finer product compared to grate-only discharge assembly.